

# Controllable Motion Diffusion Model

YI SHI, Shanghai AI Lab, China

JINGBO WANG, The Chinese University of Hong Kong, China

XUEKUN JIANG, Shanghai AI Lab, China

BO DAI, Shanghai AI Lab, China

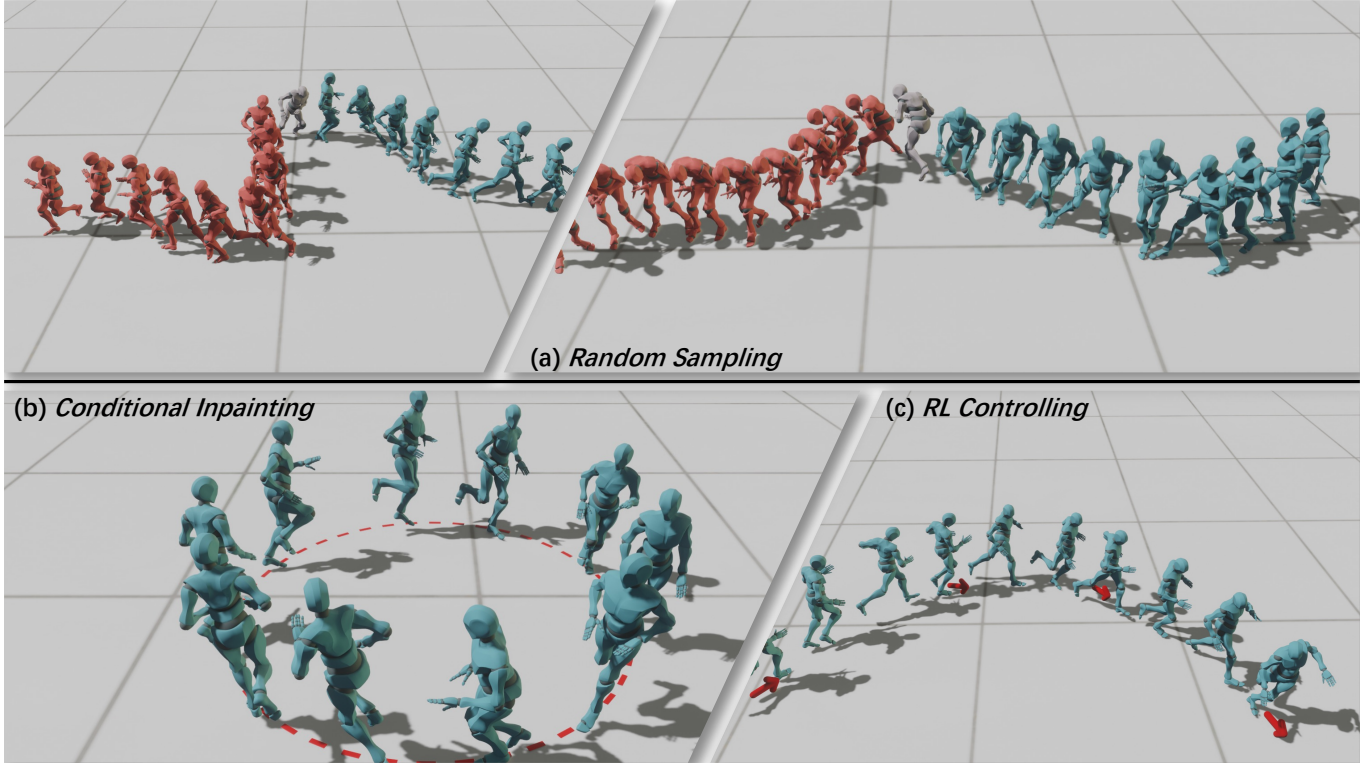


Fig. 1. We present our framework, the Controllable Motion Diffusion Model (COMODO), aimed at the sophisticated generation of diverse, prolonged, and high-fidelity motion sequences using various control strategies. Figure (a) showcases the capability of our framework, which generates a multitude of motions of varying lengths with different skills. Our framework encompasses different control strategies that ensure optimized performance, as indicated in Figures (b) and (c), including trajectory inpainting facilitated by expert demonstrations as described in [29, 35], as well as an advanced reinforcement learning (RL) based controller, respectively.

Generating realistic and controllable motions for virtual characters is a challenging task in computer animation, and its implications extend to games, simulations, and virtual reality. Recent studies have drawn inspiration from the success of diffusion models in image generation, demonstrating the potential for addressing this task. However, the majority of these studies have been limited to offline applications that target at sequence-level generation that generates all steps simultaneously. To enable real-time motion synthesis with diffusion models in response to time-varying control signals, we propose the framework of the Controllable Motion Diffusion Model (COMODO). Our framework begins with an auto-regressive motion diffusion model (A-MDM), which generates motion sequences step by step. In this way, simply using the standard DDPM algorithm without any additional complexity, our framework is able to generate high-fidelity motion sequences over extended periods with different types of control signals. Then, we propose our reinforcement learning-based controller and controlling strategies on top of the A-MDM model, so that our framework can steer the motion synthesis process across multiple tasks, including target reaching, joystick-based control, goal-oriented control, and trajectory following. The

proposed framework enables the real-time generation of diverse motions that react adaptively to user commands on-the-fly, thereby enhancing the overall user experience. Besides, it is compatible with the inpainting-based editing methods [17, 29, 35] and can predict much more diverse motions without additional fine-tuning of the basic motion generation models. We conduct comprehensive experiments to evaluate the effectiveness of our framework in performing various tasks and compare its performance against state-of-the-art methods. Project page: [ControllableMDM.github.io](https://github.com/ControllableMDM)

Additional Key Words and Phrases: Motion Synthesis, Diffusion Model, Reinforcement Learning

## 1 INTRODUCTION

The task of synthesizing high-fidelity and controllable human motions for virtual characters is a persistent and significant challenge in the field of computer animation, with broad implications for

applications such as computer games, simulations, and virtual reality. The intricate nature of human motion, encompassing a vast array of styles and tasks, presents a formidable challenge for achieving high-quality motion generation that necessitates the prowess of sophisticated generative models. In recent years, researchers have drawn on the success of data-driven methods [9, 25–27, 31] utilized in text and image generation to address this challenge, achieving promising results in quality and diversity without depending solely on manual processes of experts. Notably, as highlighted in [3, 11, 17, 23, 29, 35, 41, 44, 46, 47], diffusion model has demonstrated its potential as a powerful tool for synthesizing diverse and high-quality motions. Under ideal observed conditions, such as accurately captured language descriptions or well-designed trajectories, diffusion model-based methods have demonstrated an ability to synthesize high-quality and diverse motion. However, the applicability of these methods for real-time controlling of virtual characters, such as joystick-based and goal-oriented control, remains largely unexplored and requires further investigation.

In this paper, our objective is to explore the potential of diffusion model-based methods for synthesizing motions that can be effectively controlled on-the-fly. We propose a novel approach, the Controllable Motion Diffusion Model, for achieving this goal by combining the diffusion model with reinforcement learning techniques, drawing inspiration from prior research [16, 39] in this area. Unlike previous works [29, 35, 41], our real-time control approach requires a motion diffusion model that can generate high-fidelity motion efficiently and adaptively respond to changing control signals. To this end, we redesign the motion diffusion model, named A-MDM, in an auto-regressive form that generates motion frames incrementally, rather than generating the entire motion sequence simultaneously. Our approach forecasts the next motion frame using only 16 denoising steps, which is significantly less than the 1000 steps used in previous works [29, 35, 41] and thus can run in real-time. Thus A-MDM is suitable for real-time motion control situations with rapidly varying input signals.

Our A-MDM model serves as the foundation for developing a reinforcement learning-based controller that effectively controls the motion synthesis process across multiple tasks. In stark contrast to VAE-based works [16, 40, 43], our A-MDM requires multiple noise vectors to generate motion for the next step, without an explicit latent space. Therefore, employing samples  $z$  as action spaces is not efficient in our A-MDM model. To address this issue, we draw inspiration from the inpainting techniques utilized in [29, 35] to predict the requisite motion changes for each denoising step of our A-MDM model to satisfy the given task. Our framework combines this prediction strategy with well-defined reward functions for conditional goals to learn a robust controlling policy for virtual characters. Furthermore, our approach retains the sampling process during predicted motion in the next step to generate diverse motions while fulfilling the given task. Through experimental evaluations, we demonstrate our approach’s effectiveness in performing various tasks, including joystick-based control, goal-oriented control, and trajectory following. Furthermore, we showcase our controlling scheme’s efficiency, highlighting its potential for use in real-time applications.

Significantly, our framework demonstrates compatibility with the inpainting-based editing method, as delineated in [17, 29, 35], by enabling the injection of supplementary control features during the controlling process. In contrast to VAE-based methods that solely rely on implicit latent codes for motion, our A-MDM establishes an explicit correspondence between the noise vector and kinematics, enabling the direct editing of end effectors of motion in upcoming steps. This attribute empowers our framework to modify motion styles during goal-oriented controlling, including but not limited to raising hands or lowering heads, thus augmenting the diversity of generated motions. Notably, our approach precludes the need for fine-tuning the motion generation model and policy network, which represents a significant departure from [29].

We summarize our contributions as follows:

- We design the auto-regressive motion diffusion model, named A-MDM, to generate motion frames step-by-step, which can be used for real-time motion synthesis for time-varying goals. Our A-MDM model can generate much more diverse motions against previous VAE [16]-based methods.
- Our framework is capable to generate high-quality motions via different controlling strategies, without the finetuning like [29].
- We explore an efficient strategy to control our A-MDM model through reinforcement learning on various tasks and learn robust policies to control virtual characters.
- We integrate this RL-based controlling framework with the inpainting-method [17, 29, 35] of the diffusion model to extend the capability of our real-time motion controlling framework.

## 2 RELATED WORKS

The animation of virtual characters is a complex problem that has perplexed computer graphics researchers for some time. To address this issue, multiple approaches have been explored, including kinematics-based and physics-based techniques. Our study is firmly rooted in the kinematics paradigm, providing a pathway to generate movements that exhibit psychological realism, while sidestepping the dependencies of a physics simulator. This essential characteristic affords our model greater flexibility and adaptability for application in a multitude of instances. Our framework of controllable motion diffusion model comprises an auto-regressive motion diffusion model in conjunction with a controller network constructed to cater to a variety of tasks, ultimately culminating in an efficient and intuitive approach to motion generation.

### 2.1 Kinematics Motion Generation

Kinematics-based techniques tend to be divided into two categories: sequence-level generation and auto-regressive generation. Sequence-level generation requires the generation of an entire motion sequence in one go, whereas auto-regressive generation generates the motion sequence step-by-step, allowing greater flexibility with respect to time-varying objectives and rendering it more applicable to real-time scenarios. In this paper, we focus on the auto-regressive generation approach, which produces high-quality and realistic

motions in a real-time fashion. We will delve into both sequence-level and auto-regressive generation in our subsequent sections, reviewing the literature that exists in each field.

*Auto-regressive motion Generation.* Auto-regressive methods for generating long-term motions have been studied extensively. Early works used CNNs, LSTMs, and feed-forward networks to predict the next state in a straightforward manner [1, 4, 6, 15, 18, 19]. However, applying these methods directly often resulted in divergence or convergence to a mean pose for long-term motion generation and created unnatural human behaviors. To address these issues, researchers have introduced more innovative design choices to improve motion quality and diversity. For instance, the Phase-Functioned Neural Network [10] incorporates parameters computed by pre-defined phase functions to generate long-term, high-quality movements, though this method often results in cyclic behaviors in generated motions influenced by phase variables. To address this limitation, a more recent study [33] integrated phase variables and a mixture of experts (MoE) mechanism [45] to produce long-term human motions with object-aware interactions. Other studies have attempted to learn the motion manifold through VAEs [14]. MVAE [16] employs an MoE network structure alongside a VAE model to generate diverse motions in the next step, while Humor [24] models the manifold of transitions in two adjacent frames via VAE methodology. SAMP [8] utilizes a VAE model to synthesize long-term motions of human-scene interactions. In contrast to these works, our paper explores the first implementation of the diffusion model in auto-regressive motion generation with real-time, changing control signals. Our method delivers promising results and outperforms previous state-of-the-art approaches, such as MVAE [16].

*Sequence-level Generation.* Sequence-level motion generation techniques are typically developed for offline applications. Given well-planned controlling guidance, these methods can produce high-quality motions. Previous research has utilized convolution layers [38, 42] and transformers [13, 22, 37] in GAN [5] and VAE [14] frameworks to generate long-term motions. Recently, researchers have begun using the diffusion model [9] in motion generation, achieving promising results. MDM [35] and MotionDiffuse [46] use the diffusion model with language prompts and a transformer structure. Latent MDM [41] introduces a latent diffusion framework into motion generation, increasing the speed of the language-based motion generation model. SceneDiffuser [11] integrates the scene context into the diffusion model to generate context-aware motions. MoFusion [17] synthesizes high-quality motions under the condition of music. EDGE [36] generates high-fidelity motion sequences guided by music. PhyDiff [44] combines the diffusion model with the output of the physics imitator, generating motions that are physically plausible. In contrast to these works, our controllable motion diffusion model framework generates motions in an auto-regressive fashion and flexibly interacts with real-time controlling signals.

## 2.2 Latent-based Motion Control

Once one has become familiar with the motion manifold, generating long-term motion becomes possible by sequentially sampling

latent vectors. Therefore, for a given task, a virtual character’s motion can be generated by sampling specific latent vector sequences. MVAE [16] learns the motion manifold using a conditional variational auto-encoder (cVAE) model [30] and controls this VAE model via a controller trained by reinforcement learning (RL), that samples latent codes. ASE [20] learns the motion manifold by maximizing the mutual information between latent space and the motion at the next step in the discriminative learning procedure. Physics-aware VAE [39] integrates a physics simulator into the motion-controlling framework, similar to MVAE, and generates physically plausible human motions. ControlVAE [43] integrates a world model into the VAE framework and learns the latent space directly with physically plausible states. Recently, PADL [12] and CALM [34] follow the framework of ASE to control the virtual character using language and complex actions, respectively. In addition, DeepPhase [32] learns the structured latent space of phase functions and controls motion by predicting the latent code in such a latent space. It should be noted that these methods are designed for VAE-based or discriminative learning-based techniques and do not explore state-of-the-art generation frameworks such as the diffusion model [9]. Our method is the first to investigate RL controlling of diffusion-based motion generation by predicting the noise vector at different stages. We demonstrate that our approach yields promising results for character control.

## 3 METHOD

Our framework for controllable motion diffusion models consists of two key components: an autoregressive motion diffusion model (A-MDM) and an RL-based motion controller. The A-MDM predicts the motion at frame  $f$  based on the motion at frame  $f - 1$ . This model is optimized to synthesize long-term and high-quality human motion in real-time. To achieve task-based character control, we utilize the RL-based motion controller. Specifically, we train a controller network for each task using reinforcement learning. This allows us to generate high-quality, task-oriented motions for a wide range of applications. To further enhance the diversity and controlling flexibility of generated motions, we incorporate inpainting techniques such as those utilized in [29, 35]. These techniques enable real-time motion control and result in a more realistic and natural appearance of the generated motions. For a comprehensive understanding of our A-MDM, please refer to Section 3.1, while Section 4 and Section 5 explain our unique design for task-based character control.

### 3.1 Auto-regressive Motion Diffusion Model

In this section, we will introduce the details of our auto-regressive motion diffusion model (A-MDM). Given the motion at frame  $f - 1$ , the goal of our A-MDM is to model the distribution of possible motions at frame  $f$ . Our A-MDM is trained by supervised learning via the similar diffusion model formulation as [35]. After training this model, diverse, high-fidelity, and long-term motion sequences can be generated by sampling different noise vectors during the denoising steps of the diffusion model.

*3.1.1 Motion Representation.* Before demonstrating the details of our A-MDM model, we first explain the motion representation we used in this work. Given the initial motion  $x_0$  at the 0 frame,

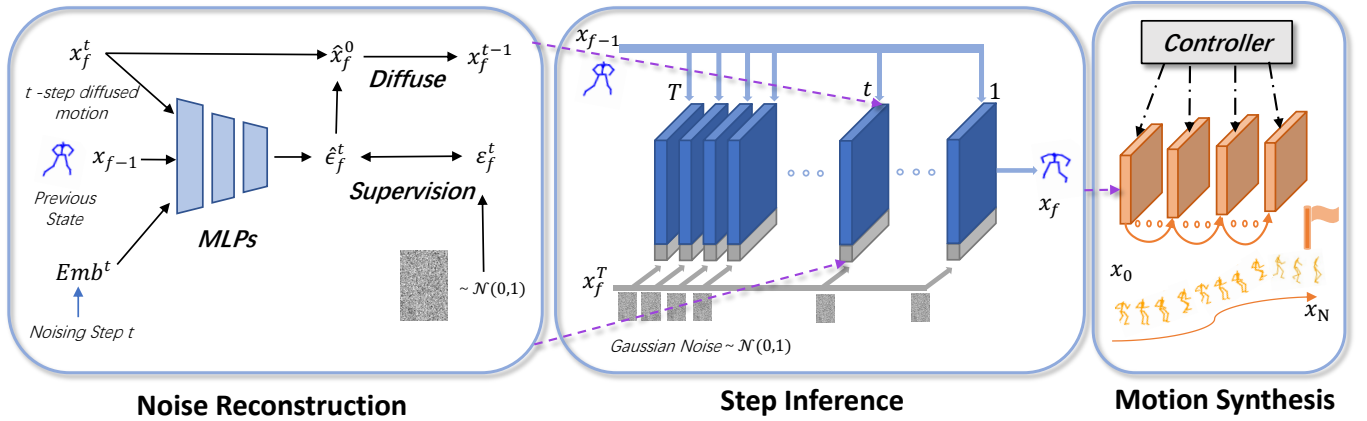


Fig. 2. **Framework of our A-MDM.** Our A-MDM is trained following DDPM [9]. During training, the goal of our A-MDM is to reconstruct the sampled noise vector  $\epsilon_f^t$  at each step. After training, our A-MDM is capable to generate motion with arbitrary lengths under different controlling strategies in an autoregressive manner.

our A-MDM is capable of generating the motion sequence  $X = \{x_1, x_2, \dots, x_F\}$  with arbitrary length  $F$  in an auto-regression manner. The motion  $x_f$  at frame  $f$  mainly consists of four main components: planar linear velocities ( $d_x \in \mathbb{R}, d_y \in \mathbb{R}$ ), angular velocity ( $d_r \in \mathbb{R}$ ) of up-axis, joint positions ( $j_p \in \mathbb{R}^{j \times 3}$ ), joint velocity ( $j_v \in \mathbb{R}^{j \times 3}$ ), and global joint orientations in 6D representation [48] ( $j_o \in \mathbb{R}^{j \times 6}$ ). Specifically,  $d_x, d_y,$  and  $d_r$  are transformed from the root orientation and root position in the world space as such incremental variables, similar to MVAE [16, 24]. Therefore, the diffusion and reconstruction processes in our A-MDM are both conducted on this tuple  $x_f = (d_x, d_y, d_r, j_p, j_v, j_o)$  during the training and inference stage.

**3.1.2 Pipeline Overview.** With a given input character motion,  $x_{f-1}$ , A-MDM predicts the potential motion of the future frame  $x_f$  in an autoregressive manner. To obtain a high-quality motion frame, A-MDM follows the procedure of DDPM[9], which includes a forward diffusion process and a backward reconstruction process. During the forward diffusion process, Gaussian noise is introduced step by step in small amounts on the future motion  $x_f$ , and there are  $T$  steps in total, until  $x_f$  is equivalent to an isotropic Gaussian noise. The backward reconstruction phase, divided into  $T$  steps, represents a reversed procedure during inference where a neural network gradually removes the noise on the condition of the input frame  $x_{f-1}$ , yielding the final prediction  $x_f$ .

During training, the forward diffusion process is performed first. Gaussian noise is added in a Markov Process on the ground truth character pose  $x_f$ . For a single forward step  $t$ , the noising process can be represented by:

$$q(x_f^t | x_f^{t-1}) = \mathcal{N}(x_f^t; \sqrt{1 - \beta^t} x_f^{t-1}, \beta^t I), \quad (1)$$

where  $\beta t \in (0, 1)$  is a hyper-parameter that decides the schedule of noise addition. The whole noising process can be formulated by equation 2.

$$q(x_f^{1:T} | x_f^0) = \prod_{t=1}^T q(x_f^t | x_f^{t-1}), \quad (2)$$

We denote the noise added on pose  $x_f$  after  $t \in (1, T)$  steps as  $\epsilon^t$ . Our reverse reconstruction process is then performed using a Neural Network  $p_\theta$ . The network takes the perturbed target motion  $x_f^t$ , which is computed by the reconstructed motion  $x_f^0$  at time step  $t+1$  and the sampled noise  $\epsilon_f^t$  from the standard Gaussian distribution, as well as the time embedding at time step  $t$  and the previous motion  $x_{f-1}$  as input, to predict the noise vector  $\hat{\epsilon}_f^t$  for noise reconstruction. We apply MSE to compute reconstruction loss between predicted noise and the ground truth  $\epsilon^t$ .

$$L_t^{simple}(x) = \mathbb{E}_{t \sim [1:T], x_f^0, \epsilon^t} \|\epsilon_t - p_\theta(x_{f-1}, x_f^t, emb^t)\|_2, \quad (3)$$

**3.1.3 Network Structure.** The primary goal of our controllable motion diffusion model framework is to control virtual characters in real time. In order to achieve this goal, the network structure of our model needs to be lightweight and possess the ability to generate high-quality motions while adhering to the real-time inference settings of the diffusion model (such as fewer denoising steps). For this purpose, we have designed a lightweight MLP-based network structure for our A-MDM model, shown in Figure 2. Our model comprises 9 fully-connected layers, with each layer having 128 hidden dimensions. The input to this model includes the motion at the previous step  $x_{f-1}$ , the perturbed target motion  $x_f^t$ , and the time embedding  $emb^t$  of the diffusion step  $t$ . Our model takes the

previous motion condition  $x_{f-1}$  as input to each layer to ensure the predictions remain within the plausible motion space. Thanks to this lightweight design choice, our model can effectively generate high-fidelity motion in real-time. Our thorough quantitative and qualitative experiments demonstrate that using MLPs in diffusion models with fewer denoising steps (such as 16 steps) is sufficient for motion synthesis, and it outperforms MVAE in both generation variety and fidelity.

### 3.2 Training and Inference

**3.2.1 Training.** As discussed in Section 3.1.2, during training our A-MDM, the loss function is the predicted noise and the sampled noise at each time step  $t$  in Equation 3 for each frame. However, as discussed in [16, 24], generating motion with an autoregressive motion decoder, which is only trained by reconstruction loss, is susceptible to failure due to cumulative errors (e.g., unreasonable poses or deforming limbs). These errors make long-term motion generation more difficult in such an autoregression manner. To overcome this hurdle, we design a rollout training phase specifically for our A-MDM model. Besides following the standard DDPM procedure for  $N_d$  epochs, we train the model for another  $N_r$  epochs with Rollout loss. Rollout is a key training phase that ensures failure-free motion generation applied in VAE-based models. In A-MDM, the entire denoising steps  $T$  are executed, and the output  $x_0^f$  of the previous frame  $f$  is fed back to the framework. The rollout loss is computed using MSE loss between ground truth  $x^f$  and  $x_0^f$ .

Despite having a better capability to produce smoothed and failure-free motion sequences, the diffusion process itself may not be sufficient for ultra-long sequence generation (>500 steps). Therefore, the rollout training is still essential, especially for task-based motion generation coordinated by RL controller which has a large control space. We also discover that using a shorter rollout step can retain more variety in the generated motion. The empirical sweet spot is between 3-4 steps for most  $T$  and network configurations.

**3.2.2 Real-time Design Choices.** The use of an autoregressive denoising method in A-MDM with large diffusion steps (e.g., 1000 steps as in DDPM) can result in time-consuming generation due to the large number of required inference steps. Therefore, we explore different strategies to speed up the diffusion process, including using large diffusion steps with DDIM [31] and directly training a model with small diffusion steps. In contrast to prior studies that used the default of 1000 diffusion steps, we empirically found using very few steps is sufficient for motion generation tasks. While it may have seemed tempting to use DDIM to speed up the diffusion process, we observe that the generated quality deteriorated and the model was unable to handle accumulated errors in the sequence.

## 4 MOTION SYNTHESIS

After training the A-MDM model, we demonstrate its ability to generate long-term motion by sampling noise vectors at each time step. We present three methods for long-term motion generation: random sampling, task-oriented sampling, and conditional inpainting. The first method involves randomly sampling noise vectors at each step and may result in less natural-looking motion. The second method generates long-term motions for a given task. The third

method uses an inpainting technique as [35] to generate long-term motions under the given condition (e.g., the trajectory condition). Furthermore, we illustrate using reinforcement learning methods on top of our A-MDM for task-oriented motion control in the next section. It is worth noting that the weights of our A-MDM model are fixed at this moment, without the finetuning in [29].

### 4.1 Synthesis via Random Sampling

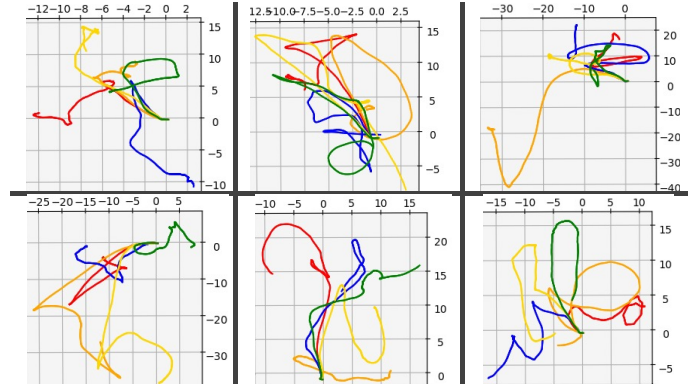


Fig. 3. **Trajectories of synthesized motions.** We show that our A-MDM model can generate motions with diverse trajectories from different initial states. More synthesized results are in our supplementary video.

Given the initial motion state, our A-MDM can generate plausible and random motion for the next time step by sampling noise vectors. This random sampling enables the generation of long-term and diverse motion sequences auto-regressively, with the output motion of the previous step as the input. The diverse trajectories of synthesized motion from different initial motions are shown in Figure 3. Besides, our supplementary video also demonstrates the capability of our A-MDM to transition from a stationary pose to various actions like walking, running, and jumping with diverse motions. Additionally, when the initial motion is a hopping pose, our A-MDM generates the hopping motion first and then transitions into other actions rather than directly changing to common motions. These examples exemplify the ability of our A-MDM model to learn the distribution of potential motions for a given state. Furthermore, our supplementary video provides additional examples of our method’s capabilities.

### 4.2 Synthesis via Task Oriented Sampling

In addition to random generation, our A-MDM is also capable of synthesizing long-term and diverse motion via goal-oriented sampling, similar to Motion VAE [16]. This task-oriented sampling involves multiple Monte Carlo roll-outs, selecting the action of the best trajectory among all sampled roll-outs, and applying it to the character as the next step for the current state. This process is repeated until the task is accomplished or terminated by other constraints.

We find that this task-oriented sampling works reasonably well for simple locomotion tasks, such as target reaching (as shown in Section 6.1). Figure 7.2.2 displays the trajectories of sampled motion for this task. Compared to Motion VAE [16], our method

can generally navigate to the target motion directly rather than producing walking around motion. However, for more complex tasks such as joystick and path following, as with Motion VAE [16], task-oriented sampling can still face difficulties. This limitation can be overcome by using reinforcement learning-based control approaches, which we will discuss in the next section.

### 4.3 Synthesis via Conditional Inpainting

Finally, we demonstrate that our A-MDM retains the capability of inpainting-based motion synthesis, as shown in [29], given a trajectory condition. This synthesis procedure allows the user to generate long-term motion following well-designed trajectories or character velocities. For example, given the motion  $x_{f-1}$  at frame  $f-1$  and the well-designed target velocity  $(d_x, d_y, d_r)$  for the next frame  $f$ , our A-MDM model can inpaint the  $j_p$  and  $j_o$  at time step  $t$  via the reconstruction process from corresponding sampled vectors. Therefore, we can synthesize long-term motion guided by the condition by repeating this process, without any other finetuning process as [29]. Compared with task-oriented sampling, this synthesis strategy is able to generate motion for some more complex tasks, such as joystick and path following. However, this inpainting-based method requires well-designed conditions and thus is not flexible and stable for real-time controlling, which always meets out-of-distribution controlling signals (e.g., large speeds during joystick controlling in Figure 9).

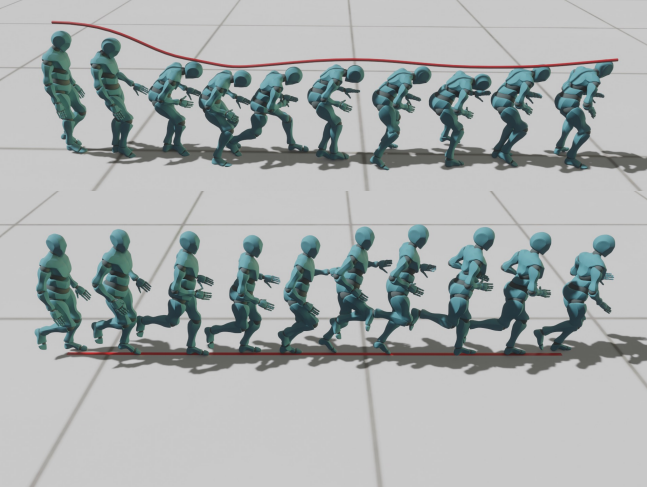


Fig. 4. **Conditional Inpainting.** Given the condition on the trajectories of head and root, our A-MDM model is capable of synthesizing high-quality motions via the inpainting techniques without additional finetuning as [29].

## 5 POLICY-BASED CONTROLLING

Beyond the synthesis procedure in Section 4, in this section, we will illustrate the policy-based approach for long-term motion synthesis, based on our A-MDM. The approach entails training an additional controller network with a carefully designed controlling strategy, which achieves more efficient training speed and greater flexibility in handling a diverse array of tasks while obviating the need

to re-train the motion generation network. After training the controller network, the proposed approach demonstrates significantly improved efficiency in accomplishing complex tasks compared to the sampling-based motion synthesis. Furthermore, empirical evidence suggests that this approach offers greater real-time stability than conditional inpainting with respect to a given task.

### 5.1 Reinforcement Learning

We use Deep Reinforcement Learning (DRL) to train stand-alone controller networks for completing more complicated tasks. In DRL, we optimize the parameters of the controller to maximize a reward evaluated by:

$$J_{RL}(\theta) = E\left[\sum_{t=0}^{\infty} \gamma^t r(s_t, a_t)\right], \quad (4)$$

where  $\gamma \in (0, 1)$  and  $r(s_t, a_t)$  represent the reward obtained if we execute the action  $a_t$  taken under state  $s_t$ . We follow the previous studies and use Proximal Policy Optimization (PPO) [28] to train the controller. A virtual character is defined as an agent. At each frame  $f$ , the agent examines the current environment observation that has been updated based on motion generated on the last frame, followed by coordinating with the basic A-MDM model to generate a new motion frame. Different from previous VAE-based approaches, our A-MDM model does not build up the latent space for the motion to the next state, thus taking the latent space as the action space is infeasible. We will illustrate the design choice on the action space of the policy network in the following Section 5.2.

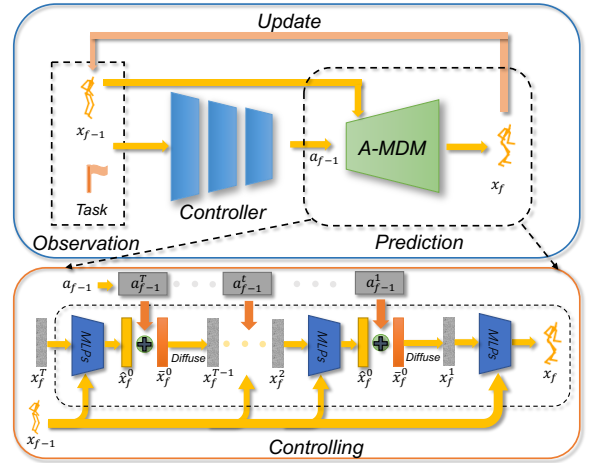


Fig. 5. The interactive mechanism between RL controller and base A-MDM model using Control by Editing. The controller predicts the moving terms introduced in the denoising steps.

### 5.2 Policy Design

Previous works [16, 39, 43] have used the latent code  $z$  as the action space for their VAE-based motion models. However, for our A-MDM model, such an action space is inefficient due to the diffusion model requiring multiple noise vectors during inference to

obtain a single motion frame. To address this, we incorporate conditional inpainting from Section 4.3 and design an action space that predicts complementary vectors for the reconstructed  $\hat{x}_f^0$  during inference while fulfilling the given task. As shown in Figure 5, the action  $a_{f-1}$  predicted by controller for the input  $x_{f-1}$  contains several vectors  $\{a_{f-1}^T, \dots, a_{f-1}^1\}$  for different diffusion steps of the A-MDM model. This prediction has explicit semantic meaning and represents the potential changes necessary for the predicted motion to accomplish the task. Our A-MDM model’s robust decoding capacity and stability empower the controller with the agility to promptly sample the necessary changes during the action selection stage. Further, coupling this with noising sampling during inference enables our approach to generate a range of diverse motions to address a specific task.

Besides, we introduce a rigid body penalty that enforces the pose fidelity and avoids failure as follows:

$$E_r = \sum_i^B \|b_i - \bar{b}_i\|^2, \quad (5)$$

where  $B$  is bone numbers of the virtual character and  $\bar{b}_i$  is the mean bone length of bone  $i$  from all training motion sequences. Besides, we also consider the effort penalty as [16] for stable results. This effort penalty energy is as follows:

$$E_e = (d_x)^2 + (d_y)^2 + (d_r)^2 + \frac{1}{J} \sum_j \|j_v\|^2, \quad (6)$$

where  $(d_x, d_y, d_r, j_v)$  is the root velocity of XY plane and up-axis, as well as the joint velocity. More details about the rewards during training the policy are explained in Section 6.

### 5.3 Combination Controlling

Additionally, we demonstrate the effectiveness of combining our policy-based controlling with conditional inpainting-based synthesis to enhance its controlling capability. For example, in the Joystick Task, as outlined in Section 6.2, we can set diverse targets for the end-effector, including the head and hands, of the virtual character being controlled. By using our A-MDM’s inpainting capabilities, we can yield other aspects of the motion states following the Joystick control. By combining these control strategies, users can create motions with varying controllable skills, including walking and then bowing their head, or running and then waving their hands. Specifically, this combination does not require finetuning the given policy network and our A-MDM model. Further details are available in the supplementary video.

## 6 LOCOMOTION CONTROLLERS

In this section, we will describe various locomotion-controlling tasks that can be achieved by RL-based policy on top of our A-MDM. Following MVAE [16], we setup up four different tasks: target reaching (Section 6.1), joystick (Section 6.2), and path following (Section 6.3) to evaluate our framework.

### 6.1 Target Reaching

Target reaching is a locomotion task in which the character is required to take maneuver toward a user-designated objective location. The coordinates of the target can be altered manually at any time regardless of the character state. A new target will be generated randomly if such changes happen or the character reaches the previous target. If the controlled character has its Hip joint falling into a 5 cm circle around the target, the target is then determined as reached. The location of a new target is restricted in a 20m×20m square area centered by the current location. In addition, we show a 3D target-reaching task that requires the character to crouch or jump to reach a target with the height requirement.

The task observation of our controller in Section 5.1 is the position of the randomly placed target  $G^*$ . For the reward of each time step, we follow MVAE [16] to compute the combination of the reward according to the distance between the new sampled state  $\dot{x}$  and  $G^*$ , as well as the progress made for reaching the  $G^*$  between  $\dot{x}$  and current state  $x$ . Besides, when the agent achieves the goal, the policy will also receive a one-time onus before a new target is set.

### 6.2 Joystick

The task of Joystick Control allows the user to specify the speed and orientation of the character. In this task, the model serves as a user-control interface for a third-person action game. The character is expected to follow user commands and display in-time and natural motion transitions between commands. We train a controller to enforce transition of varying root orientation and velocity defined by the user. In addition, we provide two extra user actions achieved by editing, a mechanism explained in 5.3. We support manually editing the height of the head and hand joints for diverse generation results.

To train the controller for this task, we simulate the joystick control by changing the desired direction and speed every 120 and 240 frames respectively. The task observation is the facing direction  $d_r^g$ , which is uniformly sampled between 0 and  $2\pi$ , as well as the desired velocity  $d_v^g$ , which is uniformly sampled from 2 and 24 feet per second. Therefore, the reward function is written as follows,

$$r = e^{\cos(d_r - d_r^g) - 1} \times e^{-|d_v - d_v^g|}, \quad (7)$$

where  $\dot{d}_r$  is the angular velocity of the sample motion in the next step and  $\dot{d}_v$  is the sampled planar linear velocity  $(\dot{d}_x, \dot{d}_y)$ . To ensure that the policy satisfies both of these objectives simultaneously, we multiply the two rewards together. This encourages the policy to maintain the right speed while also following the direction of the target point.

### 6.3 Path Following

Path following is an extension of Target reaching in Section 6.1. The character is expected to navigate along a user-defined path composed of a number of waypoints as closely as possible. The controlled character must reach each way-point in order. In detail, the task observation of our controller is the multiple targets on the pre-defined path. For practice, we set 4 target points on each spaced 15-time step. In our experiment, we train the controller on a parametric path that consists of 1200 equally-spaced steps. This path is similar to the one used in MVAE [16]. Specifically, the position

$(x_p, y_p)$  along this path is computed as follows,

$$x_p = A\sin(bt), y_p = A\sin(bt)\cos(bt), \quad (8)$$

where  $t \in [0, 2\pi]$ ,  $A = 50$ , and  $b = 2$ . To facilitate policy learning, the character’s initial state is randomly positioned on the curve, with its facing direction aligned with the path direction. We show that our method can run on novel paths after training the controller on this pre-defined trajectory.

## 7 EXPERIMENTS

In this section, we demonstrate the efficacy of our controllable motion diffusion model framework. Firstly, we evaluate the base A-MDM model and compare it with the VAE-based model (e.g., MVAE [16]) to showcase the effectiveness of our design choice for the local motion model. Following this, we present the results of controlling the A-MDM model.

### 7.1 Experiment Environment

In this paper, our framework is implemented with Pytorch 1.13.1. The experiments concerned with RL controllers are conducted using OpenAI Gym [2] and PyBullet. The model inference and time-relevant experiments are all measured on a PC with an NVIDIA GeForce 1660 Super GPU and an Intel i7-8700 CPU @ 3.20GHz. Our hardware composition represents a mediocre gaming setup, further proving that our framework has the potential to be deployed locally on time-critical applications.

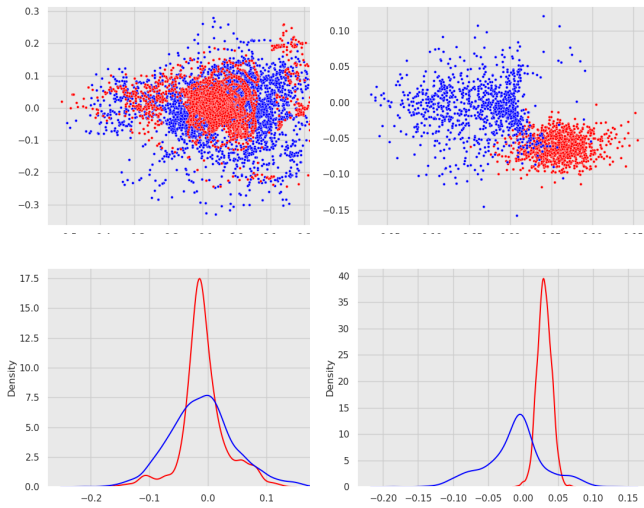


Fig. 6. Plot for linear (Up) and angular (Down) velocity distribution. Red represents MVAE and blue stands for A-MDM. We show the linear velocity on XY-plane as a 2D scatter diagram. Angular velocity is represented by a density chart.

### 7.2 Motion Synthesis

We evaluate the capability of motion synthesis in this section. We first show that our A-MDM model can synthesize much more diverse motion than the VAE-based local motion generation framework. Besides, we show that based on the potential to generate diverse motions, our A-MDM model can synthesize motion to achieve the given task much faster through sampling-based synthesis.

**7.2.1 Random Sampling.** In this evaluation, we set a fixed initial frame  $x_{f-1}$  and predict  $x_f$ . In the next step,  $x_f$  is used to generate the following motion frame. The auto-regressive process is executed for 300 steps. We run such a sampling procedure 20 times. As shown in Figure 6, we first compare the velocity distribution of synthesized motion between MVAE and A-MDM. We sample 3000 candidate frames  $x_f$  conditioned on selected initial frames  $x_{f-1}$ . We plot potential root planar movements and root angular velocity, both of which are normalized to a canonical space. On the left, the initial frame is chosen from a T-pose sequence and the left is the randomly sampled initial state from a walking cycle. For the linear velocity on XY-plane, the samples obtained using MVAE (the red one) concentrate on a central blob while the generated outcome of A-MDM (the blue one) distributes more evenly. For angular velocity, the distribution range of results (the blue one) from our A-MDM is much wider than MVAE (the red one). It illustrates that our model can generate motions with much more moving diversity. Besides, we calculate Average Pose Distance (APD) to measure its generation quality and variety quantitatively. The APD is written as follows:

$$APD(A, B) = \frac{1}{NJ} \sum_{j=1}^J \sum_{i=1}^N \|B_{ji} - A_{ji}\|_2, \quad (9)$$

where  $N$  is the number of frames, and  $J$  is the number of joints of the standard skeleton of the motion sequences.  $B_{ji}$  is the positions of the joint  $j$  of the synthesized motion at frame  $i$ , and  $A_{ji}$  is the corresponding joint positions of the ground-truth motion at frame  $i$ . As shown in Table 1, our method achieves a significantly larger APD than MVAE.

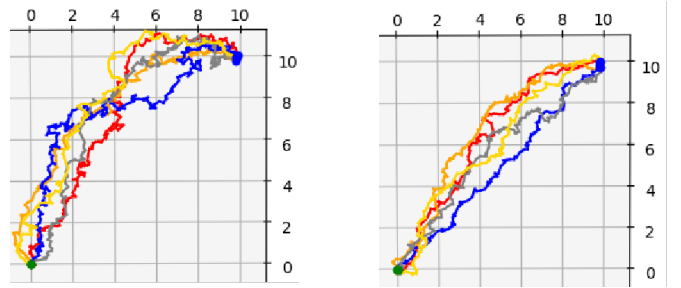


Fig. 7. Task-oriented sampling using MVAE (Left) vs. A-MDM (Right). The trajectories of A-MDM are more direct and take fewer steps.

**7.2.2 Task Oriented Sampling.** In this section, we present a comparative study of the performance of the MVAE and A-MDM models on the target-reaching task for task-oriented sampling. Specifically,



we conducted five trial runs for each base model, as depicted in distinctive colors in the accompanying figures. At each step, the base model generated 500 candidate states through random sampling, and the state that resulted in the shortest distance to the target was selected.

For this experiment, we set the target at (10 feet, 10 feet) (blue dots) and started from a fixed pose placed at the origin (green dots). Both models were trained on four locomotion clips extracted from the LaFAN1 [7] dataset, including walking, jumping, and running. MVAE followed the default MoE network and training schedule, while A-MDM used the MLP structure and a 16-step diffusion process. The trajectories displayed in the left part of Figure 7.2.2 support the findings in [16] that MVAE tends to wander around, especially when it approaches the target, while A-MDM forms more direct paths (right part of Figure 7.2.2). The reason for this lies in the larger set of movement elements that A-MDM has access to during sampling, contributing to significantly faster task completion, as shown in Figure 6.

Table 1. **Comparison with MVAE.** Our method achieves much better motion diversity and is easier to be sampled for achieving given goals.

Model	APD $\uparrow$	Avg Steps $\downarrow$	Avg Path Len $\downarrow$
MVAE	37.94	297.00	33.24
A-MDM	<b>369.92</b>	<b>165.80</b>	<b>21.43</b>

Noted motion generation using greedy search is likely to cause zig-zags in trajectories and discontinuity in limb poses with both MVAE and A-MDM, given it exhausts all possible choices along the way and selects one path which is shortest which is unnatural in sampling. Only a smooth transition between neighboring frames can be guaranteed. It can not be used as an ideal solution. Instead, it serves as a helpful evaluation metric in our study which visualizes the sampling space of an auto-regressive motion synthesizer and generalization ability. A model that can reach targets with greedy search with natural poses and trajectories would be the optimal base model that can result in ideal performance in downstream tasks.

**7.2.3 Ablation Studies.** In this section, we will explain the design choices for our A-MDM model. Firstly, we will illustrate the design choice for the diffusion step and the noise sampling strategy during inference. As shown in Table 2, we compare the different A-MDM models with different diffusion steps. With the APD for motion diversity, we also consider the Average Displacement Error (ADE), the rigid difference for motion quality, and inference time for real-time usage. For ADE,

$$ADE(A, B) = \frac{1}{NJ} \sum_{j=1}^J \sum_{i=1}^N \|B_{ji} - A_{ji}\|_2, \quad (10)$$

where  $N$  is the number of frames, and  $J$  is the number of joints of the standard skeleton of the motion sequences.  $B_{ji}$  is the positions of the joint  $j$  of the synthesized pose at frame  $i$ , and  $A_{ji}$  is the corresponding joint positions of the ground-truth motion at frame  $i$ . Rigid difference measures the average deviation of bone lengths

calculated from generated joint positions from those of a standard skeleton. We name it rigid deviation in this paper and empirically find this metric to be able to better indicate the level of authenticity and robustness of the motion synthesis model. It is able to disentangle errors of joint positions from diversity. This metric is computed as follows,

$$D_r(A) = \frac{1}{NJ'} \sum_{i=1}^N \sum_{j \in J'} \| \|A_{ij} - A_{ij_p}\|_1 - \|S_{ij} - S_{ij_p}\|_1 \|_2, \quad (11)$$

where  $J'$  is joint with parent joints. Essentially, we compare the generated bone length with the ground truth, as bone length should be a fixed rigid value. For this comparison, we randomly sample 300 steps 20 times. In this comparison, we find that the A-MDM-T16 achieves the balance of motion diversity, quality, and inference speed, and thus we choose this model as our motion generation model.

Table 2. **Diffusion Steps.** With 16 diffusion steps, our model achieves significantly better motion quality and comparable motion diversity.

Model	APD $\uparrow$	ADE $\downarrow$	Rig.Diff $\downarrow$	Inf.Time(s) $\downarrow$
A-MDM-T5	295.17	135.49	0.312	<b>0.003</b>
A-MDM-T16	369.92	<b>112.49</b>	<b>0.303</b>	0.013
A-MDM-T20	<b>370.09</b>	164.36	0.358	0.017

Next, we compare models with different layer numbers with 16 diffusion steps. We conduct this experiment on the models with 4, 6, 9, 13, and 15 MLP layers with 300 frame motion clips. In table 3, the model with 9 MLP layers achieves the balance on motion quality and inference speed. Thus, the layer number of the model in our A-MDM is 9.

Table 3. **Layer Number:** With 9 MLP layers, our framework achieves the balance of motion quality, diversity, and inference speed.

Layers	APD $\uparrow$	ADE $\downarrow$	Rig.Diff $\downarrow$	Inf.Time(s) $\downarrow$
4	289.79	182.51	0.218	<b>0.0793</b>
6	324.63	144.57	0.129	0.0990
9	<b>369.92</b>	<b>112.49</b>	0.130	0.0129
13	355.43	193.35	0.0832	0.0158
15	297.01	189.13	<b>0.0681</b>	0.021

Finally, in Table 4, we present two different strategies for achieving real-time inference and compare two common methods of acceleration. We show that applying a diffusion model with just a few steps is sufficient for auto-regressive motion generation, providing better diversity and quality. Training a model with many diffusion steps (e.g.,  $T = 200$ ) is difficult, as it requires a longer training time since rollout necessitates  $T$  denoising steps for each temporal step. Using DDIM does not offer any significant advantages, while also leading to accumulative errors. Therefore, we choose to use DDPM with fewer diffusion steps in our A-MDM. Our results demonstrate that this approach provides faster and more accurate inference, making real-time applications feasible.

Table 4. **Speeding up strategy.** We mainly compare two different strategies: using DDPM [9] with fewer steps and using DDIM [31]. Our design choice achieves the balance results under the used metrics.

Model	APD $\uparrow$	ADE $\downarrow$	Inf.Time(s) $\downarrow$	Succ $\uparrow$	Natural
T16	<b>369.92</b>	112.49	0.003	<b>30/30</b>	<b>Yes</b>
T16-I5	296.06	191.65	0.003	30/30	Yes
T16-I2	-	-	0.002	0/30	Failure
T200	281.84	<b>108.99</b>	0.174	30/30	Yes
T200-I200	305.43	120.196	0.172	30/30	Yes
T200-I20	262.57	157.59	0.021	30/30	Yes
T200-I5	219.68	109.62	0.005	30/30	Yes
T200-I1	121.12	156.93	<b>0.001</b>	25/30	Noisy.

### 7.3 Policy-based Controller

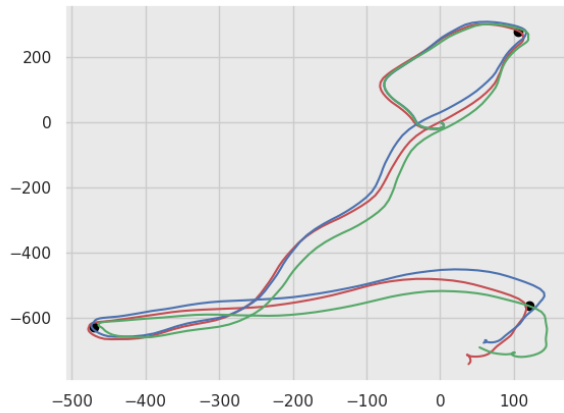


Fig. 8. **Trajectories for Target Reaching.** We show that our framework is capable to generate diverse motion trajectories, with the same initial state and target goals.

Alternatively, Deep Reinforcement Learning (DRL) provides a better solution for task-based motion synthesis. We conducted experiments on widely used locomotion tasks (see Section 6). Firstly, we compared our controlling strategy with using RL to sample the noise vector, similar to controlling VAE models [16, 39, 43]. As shown in Figure 11, learning the policy with our strategy converged significantly faster than the instinctive way of designing the action space as in VAE-based methods. Then, we showed that such an RL-based controller is much more robust to conditional inpainting for some unnatural controlling signals. For instance, as shown in Figure 9, conditional inpainting generates motion with large foot sliding for fast-moving control signals, while the RL-based method can still generate high-fidelity motions.

Furthermore, to improve the diversity of generated motions, we demonstrated the results of combination controlling. As shown in Figure 9 and Figure 10, we can control the virtual character first raise and then putting down his hand or crouching, with the

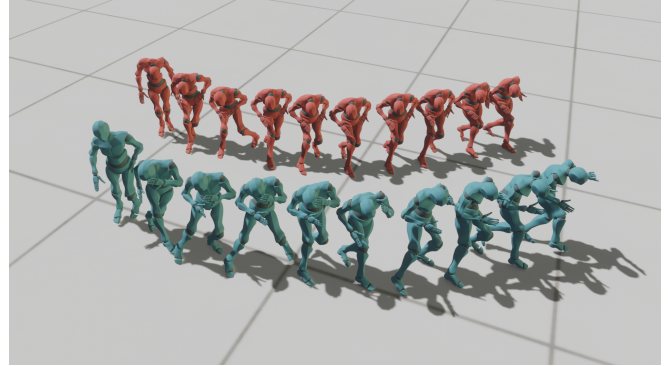


Fig. 9. **RL with conditional inpainting on the head.** We show that our policy network can work with large speeds in the joystick task (the blue one), with the given condition height on the character head. With the same condition, the speed, which is out of distribution from training data, causes much more foot sliding by directly conditional inpainting (the red one).

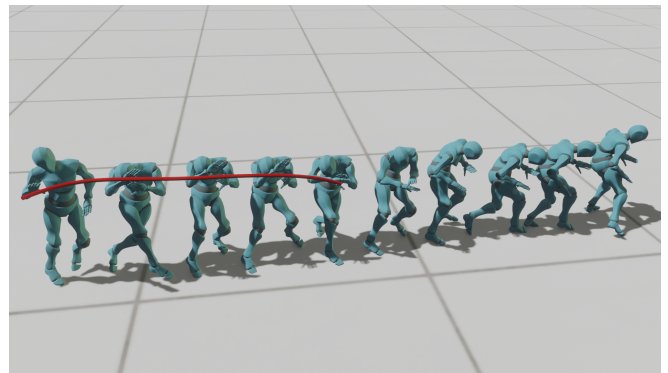


Fig. 10. **RL with conditional inpainting on the hand.** We show that our policy network is capable to work with additional given conditions.

manually given height during joystick controlling by our policy network. We also demonstrate that our method can generate diverse motions with the same initial state and controlling signal in Figure 8. These two experiments prove that our method has the potential for diverse motion generation during controlling. More details on these examples can be found in our supplementary video.

## 8 DISCUSSION

As discussed in the previous sections, we have seen a boom of research concentrated on applying the diffusion model to motion synthesis. Among these, we believe our framework is unique in its design and valuable in its application. In this section, we compare the difference and emphasize the Pros and Cons of each noticeable aspect. Finally, we explore the limitation of the model and explain our future plan for this line of studies.

### 8.1 MDM vs A-MDM

MDM [35] is a motion generation approach operating at the sequential level, exploiting a heavily-weighted transformer network.

Its success thus far has been marked primarily by its efficacy in language-based motion generation use cases, where temporal context information plays a critical role in effective synthesis. However, the model is not without its inadequacies, and its architecture’s scale, coupled with slow inference speed, hinders its potential utility. Despite claims to the contrary [41], where the model ostensibly generates 200 frames over three seconds, this feat is only accomplished through optimized parallelism conducted on pre-determined length sequences. In reality, the notion of MDM generating individual frames within a 0.03-second frame period or attaining 30 frames per second is untenable within a purely sequential model. This deficiency effectively bars MDM from functioning as an effective primary base model for controllable motion synthesis tasks, which, of course, represents our focal area of interest.

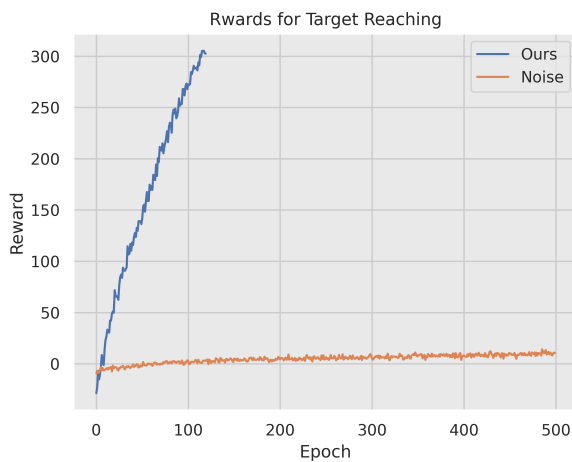


Fig. 11. **Training Curve of Target Reaching.** As illustrated in the figure, our proposed design choice significantly improves the convergence speed compared to using the policy network as sampling guidance for given tasks, similar to [16].

## 8.2 MVAE vs A-MDM

In the realm of first-order motion generation, MVAE serves as A-MDM’s equivalent counterpart. MVAE [16] distinguishes itself with its faster inference speed compared to even our most lightweight models. However, the iterative diffusion process necessary for MVAE operation multiplies the temporal computation cost, limiting its applicability in real-time scenarios. In comparison, A-MDM benefits from reduced diffusion steps and a carefully simplified network structure, enabling real-time inference while providing access to an exceptional degree of control and easier editability of results. Additionally, A-MDM boasts superior performance in diversity evaluations.

## 8.3 Limitation and Future Work

First and foremost, A-MDM is constrained by its inference speed. As such, the key to resolving this matter necessitates striking a balance between model scale and diffusion steps with optimal performance.

Doing so, however, poses additional challenges in network design while also introducing instability in generation outcomes. Second, there are issues with the training of the base model, which occurs at a sluggish pace. The extra computational expenses resulting from the iterative inference of the rollout training also exacerbate this issue. Consequently, researchers can continue devising methods to facilitate the acceleration of A-MDM model training.

For now, we haven’t explored the possibility to use A-MDM in Physically-based Motion Synthesis. We plan to apply our A-MDM model to such topics as [20, 21, 39, 43] in the future.

## 9 CONCLUSION

In our research, we present an auto-regressive diffusion model for kinematic-based motion synthesis. Unlike conventional approaches that rely on bidirectional sequential contextual data, we demonstrate that a first-order auto-regressive motion synthesis model can generate character motion with excellent stability and diversity using just a small number of training clips. To achieve real-time inference, we develop a light-weighted model and implement a variety of speed-up techniques. After training the A-MDM model, we examine different control strategies for synthesizing controllable motion sequences. We specifically devise an efficient RL-based control methodology to train the policy network for locomotion tasks and generate high-quality motions.

## REFERENCES

- [1] Emre Aksan, Manuel Kaufmann, and Otmar Hilliges. 2019. Structured prediction helps 3d human motion modelling. In *Proceedings of the IEEE International Conference on Computer Vision*. 7144–7153.
- [2] Greg Brockman, Vicki Cheung, Ludwig Pettersson, Jonas Schneider, John Schulman, Jie Tang, and Wojciech Zaremba. 2016. OpenAI Gym. [arXiv:1606.01540](https://arxiv.org/abs/1606.01540)
- [3] Rishabh Dabral, Muhammad Hamza Mughal, Vladislav Golyanik, and Christian Theobalt. 2023. MoFusion: A Framework for Denoising-Diffusion-based Motion Synthesis. In *CVPR*.
- [4] Katerina Fragkiadaki, Sergey Levine, Panna Felsen, and Jitendra Malik. 2015. Recurrent network models for human dynamics. In *Proceedings of the IEEE International Conference on Computer Vision*. 4346–4354.
- [5] Ian Goodfellow, Jean Pouget-Abadie, Mehdi Mirza, Bing Xu, David Warde-Farley, Sherjil Ozair, Aaron Courville, and Yoshua Bengio. 2020. Generative adversarial networks. *Commun. ACM* 63, 11 (2020), 139–144.
- [6] Anand Gopalakrishnan, Ankur Mali, Dan Kifer, Lee Giles, and Alexander G Ororbia. 2019. A neural temporal model for human motion prediction. In *Proceedings of the IEEE Conference on Computer Vision and Pattern Recognition*. 12116–12125.
- [7] Félix G. Harvey, Mike Yurick, Derek Nowrouzezahrai, and Christopher Pal. 2020. Robust Motion In-Betweening. 39, 4 (2020).
- [8] Mohamed Hassan, Duygu Ceylan, Ruben Villegas, Jun Saito, Jimei Yang, Yi Zhou, and Michael J Black. 2021. Stochastic scene-aware motion prediction. In *Proceedings of the IEEE/CVF International Conference on Computer Vision*. 11374–11384.
- [9] Jonathan Ho, Ajay Jain, and Pieter Abbeel. 2020. Denoising diffusion probabilistic models. *NIPS* (2020).
- [10] Daniel Holden, Taku Komura, and Jun Saito. 2017. Phase-functioned neural networks for character control. *ACM Transactions on Graphics (TOG)* 36, 4 (2017), 1–13.
- [11] Siyuan Huang, Zan Wang, Puhao Li, Baoxiang Jia, Tengyu Liu, Yixin Zhu, Wei Liang, and Song-Chun Zhu. 2023. Diffusion-based Generation, Optimization, and Planning in 3D Scenes. *CVPR* (2023).
- [12] Jordan Juravsky, Yunrong Guo, Sanja Fidler, and Xue Bin Peng. 2022. PADL: Language-Directed Physics-Based Character Control. In *SIGGRAPH Asia 2022 Conference Papers*. 1–9.
- [13] Jihoon Kim, Taehyun Byun, Seungyeon Shin, Jungdam Won, and Sungjoon Choi. 2022. Conditional motion in-betweening. *Pattern Recognition* 132 (2022), 108894.
- [14] Diederik P Kingma and Max Welling. 2013. Auto-encoding variational bayes. *arXiv preprint arXiv:1312.6114* (2013).
- [15] Zimo Li, Yi Zhou, Shuangjiu Xiao, Chong He, Zeng Huang, and Hao Li. 2017. Auto-conditioned recurrent networks for extended complex human motion synthesis. *arXiv preprint arXiv:1707.05363* (2017).

- [16] Hung Yu Ling, Fabio Zinno, George Cheng, and Michiel van de Panne. 2020. Character Controllers Using Motion VAEs. *ACM Trans. Graph.* 39, 4 (2020).
- [17] Jianxin Ma, Shuai Bai, and Chang Zhou. 2022. Pretrained Diffusion Models for Unified Human Motion Synthesis. *arXiv* (2022).
- [18] Julieta Martinez, Michael J Black, and Javier Romero. 2017. On human motion prediction using recurrent neural networks. In *Proceedings of the IEEE Conference on Computer Vision and Pattern Recognition*. 2891–2900.
- [19] Dario Pavlo, David Grangier, and Michael Auli. 2018. Quaternet: A quaternion-based recurrent model for human motion. *arXiv preprint arXiv:1805.06485* (2018).
- [20] Xue Bin Peng, Yunrong Guo, Lina Halper, Sergey Levine, and Sanja Fidler. 2022. ASE: Large-scale Reusable Adversarial Skill Embeddings for Physically Simulated Characters. *ACM Trans. Graph.* 41, 4, Article 94 (July 2022).
- [21] Xue Bin Peng, Ze Ma, Pieter Abbeel, Sergey Levine, and Angjoo Kanazawa. 2021. AMP: Adversarial Motion Priors for Stylized Physics-Based Character Control. *ACM Trans. Graph.* 40, 4, Article 1 (July 2021), 15 pages. <https://doi.org/10.1145/3450626.3459670>
- [22] Mathis Petrovich, Michael J Black, and Gül Varol. 2021. Action-conditioned 3D human motion synthesis with transformer VAE. In *ICCV*. 10985–10995.
- [23] Sigal Raab, Imbal Leibovitch, Guy Tevet, Moab Arar, Amit H Bermano, and Daniel Cohen-Or. 2023. Single Motion Diffusion. *arXiv* (2023).
- [24] Davis Rempe, Tolga Birdal, Aaron Hertzmann, Jimei Yang, Srinath Sridhar, and Leonidas J Guibas. 2021. Humor: 3d human motion model for robust pose estimation. In *ICCV*.
- [25] Robin Rombach, Andreas Blattmann, Dominik Lorenz, Patrick Esser, and Björn Ommer. 2022. High-Resolution Image Synthesis with Latent Diffusion Models.
- [26] Nataniel Ruiz, Yuanzhen Li, Varun Jampani, Yael Pritch, Michael Rubinstein, and Kfir Aberman. 2022. DreamBooth: Fine Tuning Text-to-image Diffusion Models for Subject-Driven Generation. (2022).
- [27] Chitwan Saharia, William Chan, Saurabh Saxena, Lala Li, Jay Whang, Emily L Denton, Kamyar Ghasemipour, Raphael Gontijo Lopes, Burcu Karagol Ayan, Tim Salimans, et al. 2022. Photorealistic text-to-image diffusion models with deep language understanding. *NIPS* (2022).
- [28] John Schulman, Filip Wolski, Prafulla Dhariwal, Alec Radford, and Oleg Klimov. 2017. Proximal policy optimization algorithms. *arXiv preprint arXiv:1707.06347* (2017).
- [29] Yonatan Shafir, Guy Tevet, Roy Kapon, and Amit H Bermano. 2023. Human Motion Diffusion as a Generative Prior. *arXiv* (2023).
- [30] Kihyuk Sohn, Honglak Lee, and Xinchen Yan. 2015. Learning structured output representation using deep conditional generative models. *Advances in neural information processing systems* 28 (2015).
- [31] Jiaming Song, Chenlin Meng, and Stefano Ermon. 2021. Denoising diffusion implicit models. *ICLR* (2021).
- [32] Sebastian Starke, Ian Mason, and Taku Komura. 2022. DeepPhase: Periodic autoencoders for learning motion phase manifolds. *ACM Transactions on Graphics (TOG)* 41, 4 (2022), 1–13.
- [33] Sebastian Starke, He Zhang, Taku Komura, and Jun Saito. 2019. Neural state machine for character-scene interactions. *ACM Trans. Graph.* 38, 6 (2019), 209–1.
- [34] Chen Tessler, Yoni Kasten, Yunrong Guo, Shie Mannor, Gal Chechik, and Xue Bin Peng. 2023. CALM: Conditional Adversarial Latent Models for Directable Virtual Characters. *arXiv preprint arXiv:2305.02195* (2023).
- [35] Guy Tevet, Sigal Raab, Brian Gordon, Yonatan Shafir, Daniel Cohen-Or, and Amit H Bermano. 2023. Human motion diffusion model. *ICLR* (2023).
- [36] Jonathan Tseng, Rodrigo Castellon, and C Karen Liu. 2022. EDGE: Editable Dance Generation From Music. *arXiv preprint arXiv:2211.10658* (2022).
- [37] Jingbo Wang, Yu Rong, Jingyuan Liu, Sijie Yan, Dahua Lin, and Bo Dai. 2022. Towards diverse and natural scene-aware 3d human motion synthesis. In *Proceedings of the IEEE/CVF Conference on Computer Vision and Pattern Recognition*. 20460–20469.
- [38] Jingbo Wang, Sijie Yan, Bo Dai, and Dahua Lin. 2021. Scene-aware generative network for human motion synthesis. In *Proceedings of the IEEE/CVF Conference on Computer Vision and Pattern Recognition*. 12206–12215.
- [39] Jungdam Won, Deepak Gopinath, and Jessica Hodgins. 2022. Physics-based character controllers using conditional VAEs. *ACM Transactions on Graphics (TOG)* 41, 4 (2022), 1–12.
- [40] Jungdam Won and Jehee Lee. 2019. Learning body shape variation in physics-based characters. *ACM Transactions on Graphics (TOG)* 38, 6 (2019), 1–12.
- [41] Chen Xin, Biao Jiang, Wen Liu, Zilong Huang, Bin Fu, Tao Chen, Jingyi Yu, and Gang Yu. 2023. Executing your Commands via Motion Diffusion in Latent Space. In *CVPR*.
- [42] Sijie Yan, Zhizhong Li, Yuanjun Xiong, Huahan Yan, and Dahua Lin. 2019. Convolutional sequence generation for skeleton-based action synthesis. In *Proceedings of the IEEE/CVF International Conference on Computer Vision*. 4394–4402.
- [43] Heyuan Yao, Zhenhua Song, Baoquan Chen, and Libin Liu. 2022. ControlVAE: Model-Based Learning of Generative Controllers for Physics-Based Characters. *ACM Trans. Graph.* (2022).
- [44] Ye Yuan, Jiaming Song, Umar Iqbal, Arash Vahdat, and Jan Kautz. 2022. PhysDiff: Physics-Guided Human Motion Diffusion Model. *arXiv* (2022).
- [45] He Zhang, Sebastian Starke, Taku Komura, and Jun Saito. 2018. Mode-adaptive neural networks for quadruped motion control. *ACM Transactions on Graphics (TOG)* 37, 4 (2018), 1–11.
- [46] Mingyuan Zhang, Zhongang Cai, Liang Pan, Fangzhou Hong, Xinying Guo, Lei Yang, and Ziwei Liu. 2022. MotionDiffuse: Text-Driven Human Motion Generation with Diffusion Model. *arXiv* (2022).
- [47] Mingyuan Zhang, Xinying Guo, Liang Pan, Zhongang Cai, Fangzhou Hong, Huirong Li, Lei Yang, and Ziwei Liu. 2023. ReMoDiffuse: Retrieval-Augmented Motion Diffusion Model. *arXiv* (2023).
- [48] Yi Zhou, Connelly Barnes, Lu Jingwan, Yang Jimei, and Li Hao. 2019. On the Continuity of Rotation Representations in Neural Networks. In *The IEEE Conference on Computer Vision and Pattern Recognition (CVPR)*.